Polymer 226 (2021) 123824

Contents lists available at ScienceDirect

Polymer

journal homepage: www.elsevier.com/locate/polymer

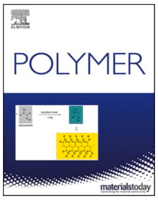

New amphiphilic semi-interpenetrating networks based on polysulfone for anion-exchange membrane fuel cells with improved alkaline and mechanical stabilities

Nieves Ureña [a], María Teresa Pérez-Prior [a], Carmen del Rio [b], Alejandro Várez [a], Belén Levenfeld [a,*]

[a] Departamento de Ciencia e Ingeniería de Materiales e Ingeniería Química, IAAB, Universidad Carlos III de Madrid, Avda. Universidad, 30, Leganés, 28911, Madrid, Spain
[b] Instituto de Ciencia y Tecnología de Polímeros (ICTP-CSIC), C/Juan de la Cierva, 3, Madrid, 28006, Spain

ARTICLE INFO

Keywords:
Anion-exchange membrane (AEM)
Ionic groups
Polysulfone
Semi-interpenetrating network (sIPN)
Alkaline stability
Mechanical stability

ABSTRACT

As considerable advance has recently been made in enhancing the conductivity of anion-exchange membranes, durability has become the critical requirement in the development of fuel cells. Such properties often develop at the expense of the other. In this work, new amphiphilic semi-interpenetrating networks composed of free polysulfone and crosslinked polysulfone are synthesized for the first time. The same nature of both polymers makes them highly compatible. The free polymer provides the hydrophobic component, whereas the crosslinked polysulfone, functionalized with trimethylammonium, 1-methylimidazolium, or 1,2-dimethylimidazolium groups, is responsible for the ionic conductivity. The compatibility between both components in the blend, improves the mechanical properties, while unaffecting the transport properties. Thus, the obtained membranes exceed the mechanical behaviour of commercial materials, even in conditions of extreme humidity and temperature. The tensile strength of these synthesized membranes can reach to relatively high values, and when compared to the commercial PSU, the difference in tensile strength can be noted to be as low as 10%. Moreover, the tensile strength and the ductility values of the crosslinked PSU are higher than those obtained with non-crosslinked PSU. Furthermore, the membranes presented in this work show a great alkaline stability (e.g. semi-interpenetrating network containing 1,2-dimethylimidazolium maintains 87% of the ionic conductivity after 14 days of treatment). Thus, these membranes provide an improvement in the durability limiting factors, in comparison to functionalized polysulfones, fulfilling the requirements to be used as electrolytes in anion-exchange membrane fuel cells.

1. Introduction

In recent years, the development of Anion-Exchange Membrane Fuel Cells (AEMFCs) has increased mainly due to the advantages that these systems present compared to the widely known Proton-Exchange Membrane Fuel Cells (PEMFCs). The alkaline medium created by the Anion-Exchange Membrane (AEM) in the fuel cell favours electrode kinetics [1], and consequently the use of expensive and noble catalysts, such as platinum, can be avoided. Therefore, non-noble metals such as silver, cobalt, and nickel [2] can be used, thus ensuring the cost reduction of the system [3].

In these fuel cells, the AEM is an indispensable element since it acts as a separator between the electrodes, and is the medium through which the transport of hydroxide ions from the cathode to the anode takes place. However, the low conductivity of AEMs (compared to that of Proton-Exchange Membranes), the introduction of CO_2 from the air to the electrolyte, in addition to their poor chemical stability against alkali attack at high temperatures [4,5], considerably decreases the performance of AEMFCs. The first problem mainly derives from the hydroxide ion size compared to the proton size [6], (the inherent lower mobility of OH^- compared to that of H^+) [7], and remains a limiting factor. The second limiting factor, the presence of CO_2, which reacts with the OH- by forming species with an ionic mobility substantially lower [4,8], could be partly mitigated by using FCs operating on pure O_2 or CO_2-free air as the oxidizer in the cathode. However, this does not mean that

---

* Corresponding author.
E-mail address: bll@ing.uc3m.es (B. Levenfeld).

https://doi.org/10.1016/j.polymer.2021.123824
Received 17 February 2021; Received in revised form 22 April 2021; Accepted 24 April 2021

Abbreviations

AEMFCs	Anion-Exchange Membrane Fuel Cells
PEMFCs	Proton-Exchange Membrane Fuel Cells
AEM	Anion-Exchange Membrane
PPO	Poly(2,6-dimethyl-1,4-phenylene oxide)
PS	Polystyrene
PAEK	Poly(arylene ether ketone)
PVA	Poly(vinyl alcohol)
PSU	Polysulfone
QP	Quaternary phosphonium
Gua	Guanidinium
QA	Quaternary ammonium
Im	Imidazolium
PAE	Poly(arylene ether)
SD	Swelling Degree
PVBC	Poly(vinylbenzyl chloride)
PVAc	Poly(vinyl acetal)
sIPNs	Semi-Interpenetrating Networks
PEG-PAGE	Poly(ethylene glycol)-co-poly(allyl glycidyl ether)
DCL	Degree of Crosslinking
SPEEK	Sulfonated poly(ether ether ketone)
TMA	Tetramethyl ammonium
MIm	1-methylimidazolium
DMIm	1,2-dimethylimidazolium
TMEDA	*N,N,N′,N′*-tetramethylethylenediamine
NMP	1-methyl-2-pyrrolidone
DMSO-d_6	Dimethyl sulfoxide-d_6
CMPSUs	Chloromethylated Polysulfones
DC	Degree of Chloromethylation
R.T	Room temperature
^{1}H NMR	Proton Nuclear Magnetic Resonance Spectroscopy
FTIR	Infrared Spectroscopy
FE-SEM	Field Emission Scanning Electron Microscopy
TGA	Thermogravimetric Analysis
T_{OD}	Onset Decomposition Temperature
T_{FD}	Fastest Decomposition Temperature
WU%	Water Uptake
IEC	Ion-Exchange Capacity
EIS	Electrochemical Impedance Spectroscopy
(σ_m)	Membrane Ionic Conductivity
TS	Tensile Strength
HFA	High Frequency Arc
LFA	Low Frequency Arc
DMA	Dynamic mechanical analysis
PS-co-DVB	Poly(styrene-*co*-divinylbenzene)

carbonation has a null effect on AEMFC behaviour. On the other hand, the chemical stability, in adverse operating conditions, can be maximized by improving the structure of the polymeric membrane. Recently, many research works have been focused on the synthesis of novel membranes in order to improve their hydroxide conductivity [9], as well as their alkaline stability [10,11]. Polymer backbones such as poly(2, 6-dimethyl-1,4-phenylene oxide) (PPO) [12], polystyrene (PS) [13], poly(arylene ether ketone) (PAEK) [14], poly(vinyl alcohol) (PVA) [15], or polysulfone (PSU) [16,17] have been extensively used to prepare AEMs. These polymers can be easily functionalized by using cationic groups such as quaternary phosphonium (QP) [18,19], guanidinium (Gua) [20,21], quaternary ammonium (QA) [12,22], or imidazolium (Im) [23–25] which are responsible for making the backbones conductive. Although highly functionalized polymers are expected to yield high conductivity, the presence of a great number of cationic groups, covalently bonded to the polymer chain, may cause the membrane to be brittle [26]. This is the case for PSU, which is a thermoplastic engineering polymer. The use of this polymer, as a backbone in the synthesis of AEMs, has been extensively reported in the literature due to its high thermal stability, good chemical resistance, and excellent mechanical properties. Moreover, PSU has two activated positions per repeat unit where an electrophilic aromatic substitution can take place, leading to high degrees of functionalization [16,17,27].

One strategy to improve the chemical and mechanical stability of the AEMs is through the development of new polymeric backbones containing copolymers based on random or hydrophobic/hydrophilic block structures. In particular, by varying the monomer units, Chu et al. developed a series of poly(arylene ether) (PAE) random copolymers whose ionic conductivity was retained at 97% after 700 h in a 2 M KOH solution at 70 °C [28]. Following another approach, Cha et al. prepared a copolymer composed of poly(*p*-phenylene) and PAE which were reported to be stable during 7 days in a NaOH solution showing no remarkable decrease in conductivity ($\sigma = 36$ mS cm^{-1} at 25 °C) [22]. Both approaches require pure monomers. This implies that anhydrous conditions (often costly) is required throughout the entire synthesis process [29]. A simpler approach to synthetize robust polymer backbones is based on crosslinked polymers. These structures show an acceptable swelling degree (SD) which enhances their dimensional stability. For this reason, Lu et al. [30] synthesized a crosslinked AEM, based on poly(vinylbenzyl chloride) (PVBC) that was used as the hydroxide conducting polymer, while poly(vinyl acetal) (PVAc) containing dimethylamino groups was used as the macromolecular crosslinked unit. PVAc also played the role of the supporting matrix due to its good flexibility and film forming nature. The obtained crosslinked membranes presented high hydroxide conductivity, and effective membrane swelling suppression at elevated temperatures. However, when the membranes were evaluated in a 1 M KOH solution at 40 °C, the hydroxide conductivity decreased gradually from the first 48 h of testing, suggesting a very low chemical resistance.

The advantages of using polymer crosslinking can be optimized by using Semi-Interpenetrating Networks (sIPNs) instead. Unlike in polymer crosslinking, where both polymers are crosslinked, sIPNs are polymer blends composed of two or more polymers of which only one is crosslinked [31]. As a result, each polymer contributes with one or more potent properties, which, when combined, lead to an overall improved and optimized material. Thus, Pan et al. [5] prepared a sIPN composed of PPO modified with QA responsible for the membrane ionic conductivity, and poly(ethylene glycol)-co-poly(allyl glycidyl ether) (PEG-PAGE) which was used as the crosslinked component. The addition of the flexible network sharply increased the flexibility of the linear QAPPO membrane. Elongation and break of sIPN membranes in a hydrated state reached a value of 93.4% with a high mechanical strength (17.4 MPa). By optimizing the blend proportions, the authors reported that high hydration numbers increase the SD (25.5% at 80 °C), decrease the OH$^-$ concentration, and effectively enhance the ion mobility in these AEMs. In these systems, the degree of crosslinking (DCL) must be adequate to guarantee that membranes show good mechanical properties since low percentages of crosslinking increase the SD which deteriorates the mechanical stability of the membrane [32]. Kanakasabai et al. demonstrated that the degree of crosslinking of the blends composed of sulfonated PVA and sulfonated poly(ether ether ketone) (SPEEK) was an essential factor in determining the optimum properties for the blends. The 70/30 crosslinked polymer/free polymer ratio showed the highest values of ionic conductivity, mechanical strength, and thermal stability with low water uptake [33].

Among the functional groups used in AEMs, tetramethyl ammonium (TMA) has been widely used in sIPNs [5,34]. In the last years however, Im-based AEMs have brought attention to their higher ionic conductivity compared to TMA-based AEMs. In addition, the charge delocalization in the imidazolium group could avoid a hydroxide attack due to the resonance effect, described in Ref. [21] with the TMA group. Therefore, it is expected that the chemical stability of these groups is high. Based on this, Lin et al. [35] prepared crosslinked AEMs based on Im-type ionic liquids with 1-vinyl-3-methylimidazolium iodide, styrene, and acrylonitrile. The resulting membranes exhibited high ionic conductivity and good chemical stability up to 400 h in an alkaline solution, without affecting in the properties of the membranes. However, the degradation of Im-AEMs was previously reported [36] when extreme conditions, as low as 10% RH, were used.

Along this line, a sIPN composed of PSU and functionalized PSU is proposed in this work to prepare, by means of a simple method, amphiphilic membranes for AEMFCs. PSU, used as a linear polymer, was

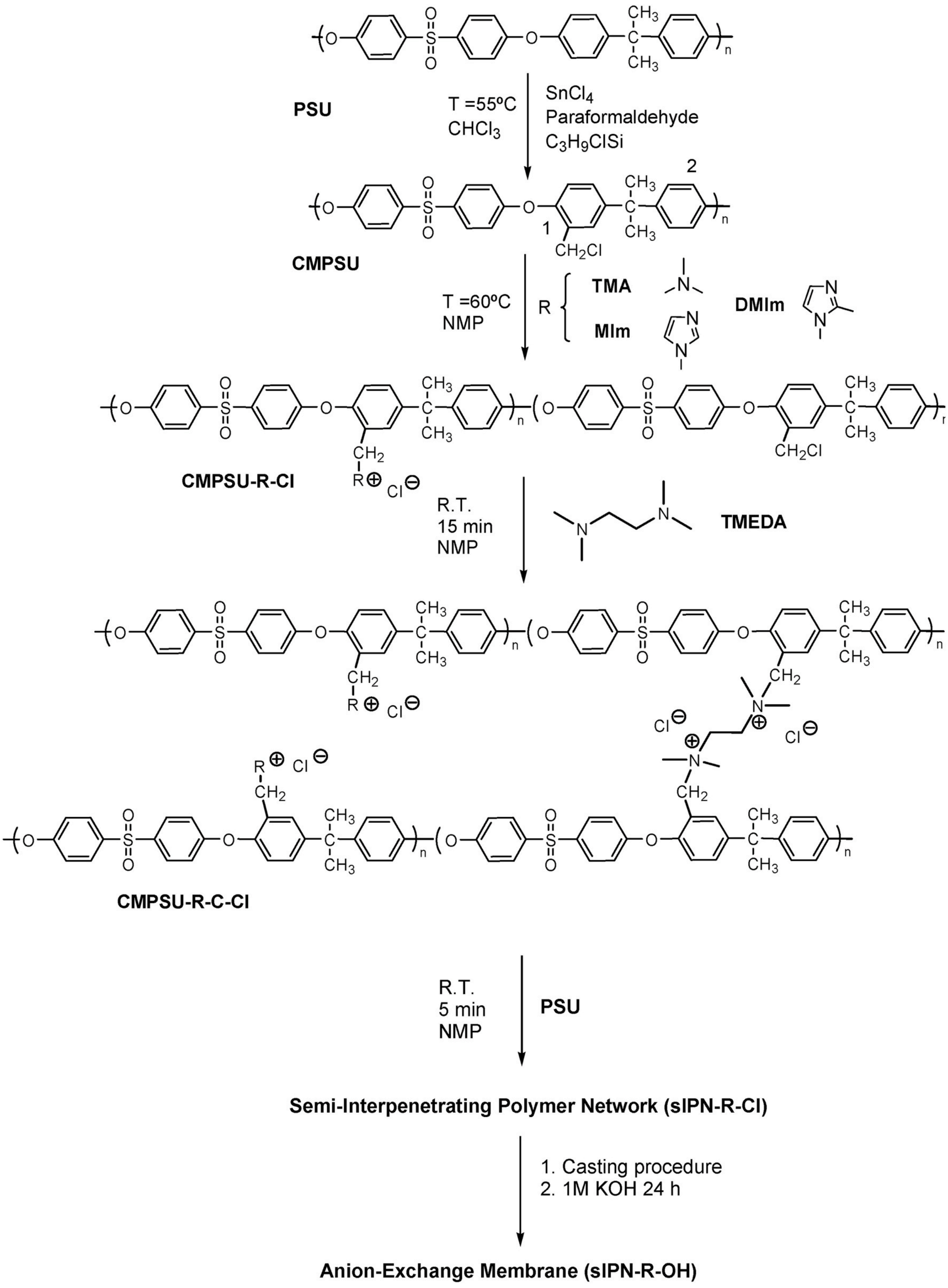

Scheme. 1. Synthesis of AEMs based on sIPNs.

homogeneously dispersed within a covalently crosslinked PSU, where cationic groups like TMA, 1-methylimidazolium (MIm), or 1,2-dimethylimidazolium (DMIm) act as a functional group, and *N,N,N′,N′*-tetramethylethylenediamine (TMEDA) as a crosslinking agent. The use of the same polymer for both segments (crosslinked and free polymers) is expected to improve the compatibility of the blend. The linear polymer contributes to improving the mechanical behaviour of the membrane, whereas the functionalized polymer is responsible for the membrane ionic conductivity, while maintaining its mechanical and dimensional stability due to the crosslinking. The mechanical properties of exchange membranes strongly affect the fuel cell performance and operating life, which are limited by the presence of high pressure reacting gasses [37]. In this sense, membranes with high strength and strain are required in order to extend the life of the membrane. sIPNs are good candidates for overcoming this limitation. In the present paper, a complete characterization of the synthesized membranes based on sIPNs, which comprises mainly of the thermal and alkaline stabilities, as well as the electrochemical and mechanical properties, is performed.

2. Experimental section

2.1. Materials and reagents

Polysulfone Udel® (22000 g mol^{-1}), tin (IV) chloride (99.0%), paraformaldehyde (95.0–100.5%), chlorotrimethylsilane (≥98.0%), chloroform (≥99.0%), 1-methyl-2-pyrrolidone (NMP) (ACS reagent, ≥ 99.0%), *N,N,N′,N′*-tetramethylethylenediamine (TMEDA) (≥99.5%), trimethylamine solution (25 wt % in H_2O), 1-methylimidazole (≥99.0%), 1,2-dimethylimidazole (98.0%), and dimethyl sulfoxide-d$_6$ (DMSO-d_6) (99.9% D) were purchased from Sigma-Aldrich. All the other reagents were of analytical grade.

2.2. Synthesis of semi-interpenetrating networks (sIPNs)

2.2.1. Synthesis of chloromethylated polysulfones (CMPSUs)

PSU was chloromethylated using the mixture of paraformaldehyde/chlorotrimethylsilane similar to the experimental procedure previously described [16,17,27,38] (Scheme 1). Thus, the use of chloromethyl methyl ether as chloromethylating agent is avoided since it is considered to be carcinogenic. In a three-neck round bottom flask, PSU (5.00 g) was dissolved in chloroform (250 mL) and subsequently stannic chloride (0.27 mL), paraformaldehyde (6.79 g), and chlorotrimethylsilane (28.64 mL) were added to the solution, where the latter was introduced dropwise. The resulting solution was maintained at 55 °C under constant and continuous mechanical stirring and during a period of time that ranged from 24 h to 72 h. The degree of chloromethylation (DC) of PSU can be easily controlled by means of the reaction time. Thus, mono-substituted PSUs (DC ≤ 100%) can be synthesized when $t < 48$ h, whereas di-substituted compounds (DC > 100%) can be obtained when $t > 48$ h. Resulting CMPSU was precipitated into ethanol, washed with deionized water, and finally dried at room temperature (R.T).

2.2.2. Synthesis of membranes based on sIPNs

As shown in Scheme 1, dried CMPSU was dissolved in NMP (6 mL) and placed in a round-bottom flask. Next, the N-compound (trimethylamine, 1-methylimidazole, or 1,2-dimethylimidazole) was added gradually to the flask (flask 1) to obtain the functionalized polymer (CMPSU-R-Cl). The percentage of functional groups in the unit of repetition ranged from 80 to 95% (100% was also used as a reference material) in order to leave some free chloromethyl groups in the polymer chain. The reaction mixture was kept at 60 °C for 3 h. Crosslinked structures were synthesized using TMEDA as a crosslinking agent. Thus, different amounts of TMEDA were added into the polymer solution (which contains free chloromethyl groups) in order to obtain a DCL between 5% and 20%. The mixtures were maintained at R.T. for 15 min in order to favour the formation of crosslinked structures (CMPSU-R-C-Cl).

In another round-bottom flask (flask 2), PSU was dissolved in NMP. Subsequently, solutions of flasks 1 and 2 were mixed at different CMPSU-R-C-Cl/PSU ratios of 9/1, 7/3, and 6/4. These mixtures (a total mass of 1 g, and a total volume of 12 mL) were stirred for 5 min, cast onto a flat glass plate, and dried in an oven (under N_2 atmosphere in order to obtain the membrane in the chloride form sIPN-R-Cl). This obtained membrane was then immersed in a 1 M KOH solution for 24 h in order to replace Cl^- with OH^- (sIPN-R-OH).

The membranes prepared in this work are described in Table 1. The effects on the properties of the membrane due to (i) the chemical structure of the cationic groups used as functional groups, (ii) the degree of chloromethylation of PSU, (iii) the degree of crosslinking, and (iv) the crosslinked polymer/free PSU ratio have were evaluated. The set of combinations of these parameters, relevant to the prepared membranes, are presented in Table S1 of the Supporting Information. Membranes with imidazolium groups were prepared considering combinations of the parameters that worked the best to yield the most desirable sIPN-TMA-OH membranes.

3. Measurements

3.1. ^{1}H NMR and FTIR analysis

^{1}H NMR spectra were registered at 300 MHz on a Bruker Avance DPX-300 spectrometer using DMSO-d_6 as the solvent. TMS was used as the internal reference.

FTIR spectra of the membranes were obtained on a PerkinElmer Spectrum GX Instrument with a wavenumber resolution of 4 cm^{-1}, a spectral range of 4000–400 cm^{-1}, and 16 scans. The spectra are shown in the supporting information (Fig. S1).

3.2. Field emission scanning electron microscopy (FE-SEM)

The morphology of membranes was characterized by FE-SEM using a FEI TENEO-LoVac equipped with an energy-dispersive detector (EDS-EDAX). SEM images were recorded operating at 5–10 kV. The representative images are shown in the supporting information (Fig. S2).

3.3. Thermogravimetric analysis (TGA)

The thermogravimetric analysis of the membranes was performed in a Pyris TGA1 instrument from PerkinElmer. The samples (~10.0 mg) were heated from 40 to 600 °C at a rate of 10 °C min^{-1} under air atmosphere. The thermal degradation of TMA, MIm and DMIm groups in the membranes was characterized through the temperature at which the weight loss starts (Onset Decomposition Temperature, T_{OD}) and the temperature of the maximum weight loss rate (Fastest Decomposition Temperature, T_{FD}).

3.4. Water uptake (WU%)

The ability of membranes to absorb water was tested by means of WU

Table 1
Properties of the prepared AEMs based on sIPNs.

Membrane	Cationic group	DC [a] %	DCL [b] %	Crosslinked polymer/PSU [c]
sIPN-TMA-OH	TMA	58, 80, 111, 118, 130 143	0, 5, 10, 15, 20	6/4 7/3 9/1
sIPN-MIm-OH	MIm	80, 100, 143	0, 5, 15	6/4 9/1
sIPN-DMIm-OH	DMIm	80, 143	0, 5, 15	6/4 9/1

[a] Degree of chloromethylation.
[b] Degree of crosslinking.
[c] Total mass = 1 g.

%. Membranes in the Cl^- form were dried at 60 °C for 24 h under vacuum. The dried membranes were immersed in a 1 M KOH solution during 48 h at room temperature, they were then washed with deionized water, and finally they were weighed. This process was systematically done three times for each sample. WU% was calculated according to the following equation [16,39].

$$WU\% = \frac{m_{h(OH)} - m_{d(Cl)}}{m_{d(Cl)}} \cdot 100 \tag{1}$$

where $m_{d(Cl)}$ and $m_{h(OH)}$ are the mass of the dried and hydrated samples, respectively.

3.5. Ion-exchange capacity (IEC) and ionic conductivity

The standard back titration method [40] was used to determine the IEC of the membranes. Firstly, dry membranes in their OH^- form were treated with a known and excessive amount of a 0.1 M HCl standard solution for 48 h. The resulting solutions were then titrated with a standardized 0.1 M KOH solution. The membranes were washed and immersed in deionized water for 24 h to remove any residual HCl, and then dried at 60 °C for 24 h and finally weighed to determine the dry mass. The titrations were repeated three times per sample. The IEC (mmol g^{-1}) of the membranes were obtained by using the following equation:

$$IEC = \frac{n_{i(H^+)} - n_{f(H^+)}}{m_{dry(Cl)}} \tag{2}$$

where $n_{i(H^+)}$ and $n_{f(H^+)}$ are the number of moles of H^+ determined before and after the neutralization in the HCl solution, respectively. While $m_{dry(Cl)}$ is the dry mass (g) of the membrane in the Cl^- form.

Ionic conductivity (σ_m) was measured by electrochemical impedance spectroscopy (EIS) using a Solartron 1260 impedance analyser, interfaced with Solartron 1287. A four-point test cell, previously described [41], was used. This test cell has two Ag/AgCl and two graphite electrodes as reference and working electrodes, respectively [16]. Measurements were carried out, using different KOH concentrations (from 10^{-4} to 10^{-1} M), over a wide range of frequency (from 10^{-1} to 10^6 Hz) with an amplitude sinusoidal wave perturbation of 10 mV and the temperature range (from 30 to 80 °C) was controlled in a Binder KMF 115(E5.2) chamber. Bode plots were used to determine the frequency region where the impedance is independent of the frequency. Afterwards, the ionic resistance was obtained from the associated Nyquist plot. The ionic conductivity was obtained from the following equation:

$$\sigma_m = \frac{L}{R \cdot A} \tag{3}$$

where σ_m is the membrane ionic conductivity (mS cm^{-1}), L (cm) is the thickness, R (Ω) is the ohmic resistance and A (cm^2) is the experimental area of the membranes.

The total mass of the polymer in the sIPNs membranes is ~1 g.

Prior to testing, the membrane was immersed in a 1 M KOH solution for 24 h to replace Cl^- with OH^-, subsequently the sample was dipped in the less concentrated solution (10^{-4} M KOH solution) during 24 h.

3.6. Alkaline stability

An alkaline stability test was carried out by immersing the membranes into a 1 M KOH solution for different periods between 24 and 120 h. Each 24 h, the membranes were taken out, and the residual KOH was removed with deionized water. The possible degradation of the functionalized polymer was monitored, as previously mentioned, by measuring the ionic conductivity at a given KOH solution and at room temperature.

3.7. Mechanical properties

The mechanical properties (tensile stress-strain tests and dynamic mechanical analysis) were evaluated using a dynamo mechanical analyser (TA Instruments, DMA Q800). The average tensile strength and elongation, at break values of the membranes in the Cl^- and OH^- form in different hydration conditions, were determined by testing three different samples of each membrane at 30 °C. The tests were performed in a controlled force mode with a stretch rate of 0.30 N min^{-1} at 1 Hz. An initial static force of 0.15 N was applied. The tensile strength (TS) is taken as the stress value at the maximum of the nominal Stress-Strain curve. For the dynamic mechanical analysis, the storage modulus (E′), loss modulus (E″), and loss tangent (tan δ) were measured from 30 to 250 °C at a heating rate of 2 °C min^{-1}. The dynamic mechanical behaviour of the membranes in the Cl^- form in dry conditions (at 60 °C for 24 h), and in the OH^- form in hydrated conditions (24 h in deionized water) was evaluated on samples of 2.5 mm width, 10 mm length, and 50 μm thickness.

4. Results and discussion

4.1. Strategy

The requirements, in order to obtain AEMs that exhibit high conductivity and elevated alkaline and mechanical stability can be summarized as follows: (i) a chemically stable functional group, and (ii) a robust polymer structure with a moderate water absorption capacity. Membranes containing an unstable chemical structure could be degraded with time due to the presence of the alkaline medium found in fuel cells. Furthermore, an elevated number of functional groups induces stiffness, which has a negative influence on the membrane durability. Therefore, in order to take these two aspects into consideration, the aim of this experimental work is focused on the synthesis of AEMs based on sIPNs, whose complex structure satisfies these essential conditions, i.e., high chemical and thermal stability which in turn contribute to the ionic conductivity, and mechanical conditions found in these electrochemical devices. This approach is based on the design of a network composed of compatible polymers; one of them is highly functionalized whose cationic groups are responsible for the OH^- conduction as well as for the control of the alkaline stability, whereas the other is non-functionalized polymer helps to improve the mechanical stability of the structure.

4.2. Synthesis of membranes based on sIPNs

The synthetic route of the sIPN-R-Cl is outlined in Scheme 1. It comprises of four steps: (i) chloromethylation of PSU, (ii) functionalization of PSU by the incorporation of TMA, MIm, or DMIm groups, (iii) crosslinking of these polymers using TMEDA as a crosslinking agent, and (iv) preparation of the sIPN by means of the mixture of free PSU and the crosslinked PSU solutions. The presence of the polymers in the sIPN and the composition-dependent behaviour are checked by preparing different sIPN-TMA-OH membranes with the purpose of optimizing the parameters. The best combinations of the parameters are selected to prepare sIPN-MIm-OH and sIPN-DMIm-OH membranes.

The degree of **chloromethylation of PSU** is determined by ^1H NMR (Fig. 1) [16,17,27]. The peak associated with the protons of the chloromethyl group (H_6) appears at 4.6 ppm, demonstrating that the reaction is carried out successfully. The degree of chloromethylation of PSU can be easily obtained through the peak areas of the protons of the chloromethyl group and that of the aromatic ring (H_1), which remain unchanged after the electrophilic reaction occurs, as follows:

$$DC = \frac{2A(H_6)}{A(H_1)} \cdot 100 \tag{4}$$

where $A(H_6)$ and $A(H_1)$ are the integral area of the H_6 and H_1 peaks,

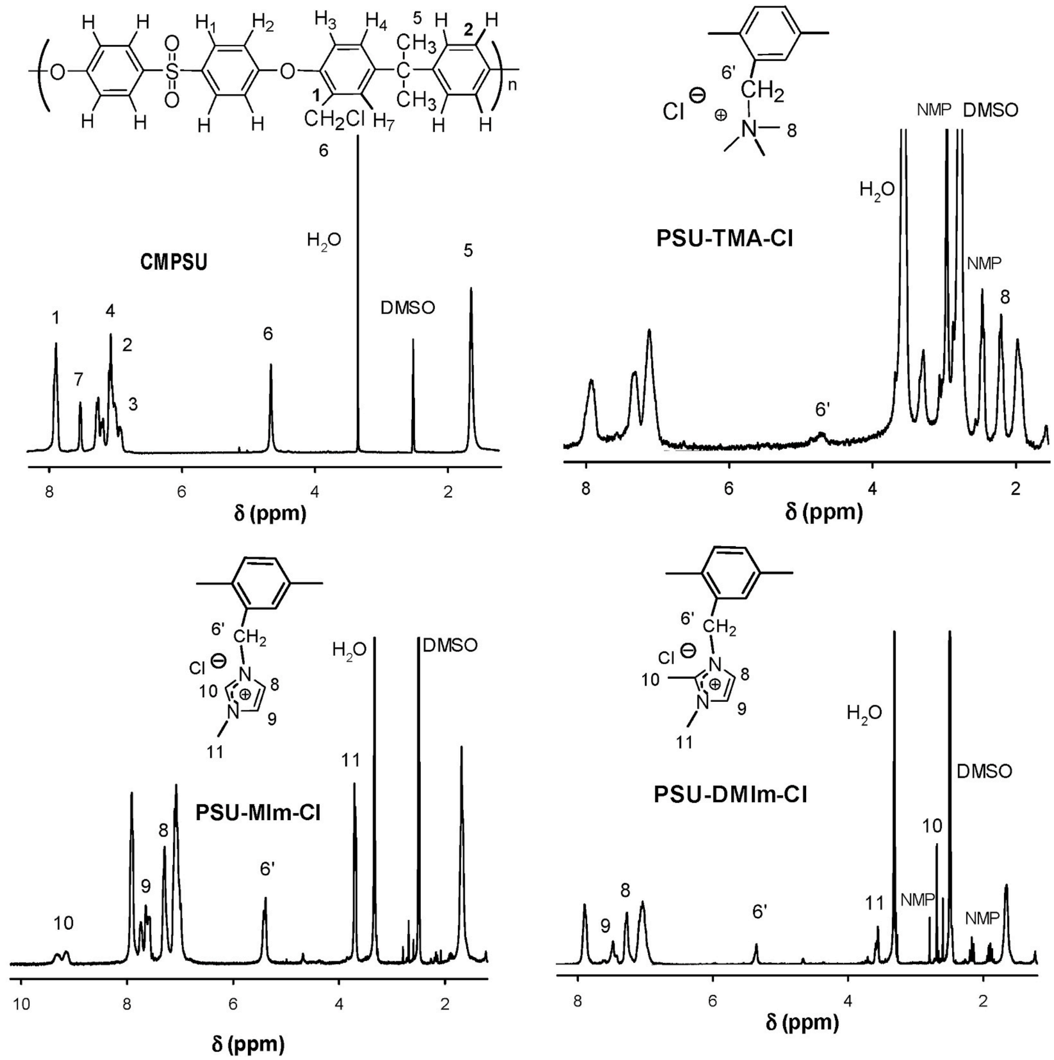

Fig. 1. ^1H NMR spectra of CMPSU and PSU modified with TMA, MIm or DMIm, respectively (Solvent: DMSO-d_6).

respectively.

Before polymer crosslinking, the **functionalization** of CMPSU with TMA, MIm, or DMIm groups is also confirmed by ^1H NMR (Fig. 1). Thus, a series of functionalized PSUs with different DC values of the original PSU (from 40 to 143%) are prepared. FTIR analysis also confirms the presence of functional groups in the polymer (see Fig. 1).

The last step in the membrane synthesis is the crosslinking by using the TMEDA agent. Unfortunately, the crosslinked polymers cannot be analysed by means of ^1H NMR, since it is not possible to solve them. Therefore, FTIR was used in order to confirm the presence of functional groups in the sIPN membranes. In Fig. S1 of the Supporting Information, pristine PSU is compared with sIPN-MIm-Cl. The presence of imidazolium groups in the sIPN-MIm-Cl spectrum is confirmed by the appearance of the band at 1680 cm^{-1}, and the shoulder at 1560 cm^{-1}, which are assigned to the imidazolium moiety anchored to the backbone [42, 43]. The spectrum also displays a broad band at 3360 cm^{-1} due to water absorption of the membranes, indicating the successful functionalization of the PSU with the imidazolium cation. No significant differences between the spectra of PSU and sIPN-MIm-Cl are observed in the other regions of the spectra due to the presence of commercial PSUs in both samples.

4.3. Thermogravimetric analysis

In order to evaluate the thermal stability of the membranes, a thermogravimetric analysis is performed. Fig. 2 shows the TGA curves of sIPN-MIm-OH and sIPN-DMIm-OH membranes with a DC lower than 100% and a DCL of 5%, and sIPN-TMA-OH with a DC = 100% and a DCL = 20%. The crosslinked polymer/PSU ratio in these membranes is 6/4. Three weight losses can be observed in the TGA curves. The first weight loss from 40 to 150 °C is due to the adsorbed water. The weight loss between 150 and 350 °C corresponds to the decomposition of the functional groups as well as the degradation of the diamine used as a crosslinking agent [44]. The third one at temperatures higher than 350 °C is due to the degradation of the polymer backbone.

Focusing on the degradation of the cationic groups, the onset and fastest decomposition temperatures are used to evaluate the influence that the cationic group has on the thermal behaviour of membranes (Table 2). The membranes composed of TMA and MIm show a similar T_{OD} (~155 °C). However, the T_{OD} for sIPN-DMIm-OH is higher (by nearly 25 °C). As shown in a previous work [45], imidazolium groups are thermally stable. Increasing the substitution of the imidazolium ions (e.g. with methyl substituents) increases the thermal stability. Therefore, it could be directly related to the thermal decomposition of the ring. Thus, the presence of two bulky methyl groups in the DMIm group makes its thermal degradation mechanism more complex [42,46]. Nonetheless, it is seen that all sIPN membranes are thermally stable at temperatures higher than 100 °C under nitrogen atmosphere.

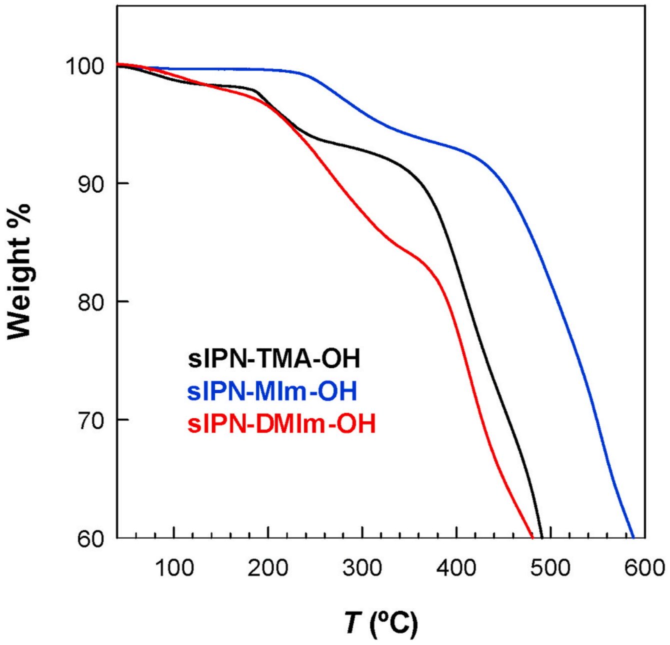

Fig. 2. TGA curves of functionalized-sIPN membranes in the OH^- form under nitrogen atmosphere.

Table 2

Onset (T_{OD}) and fastest (T_{FD}) decomposition temperatures of the membranes prepared with different functional groups under N_2 atmosphere.

Membrane	T_{OD} (°C)	T_{FD} (°C)
sIPN-TMA-OH	155	200
sIPN-MIm-OH	155	257
sIPN-DMIm-OH	180	230

4.4. Water uptake (WU%) and ion exchange capacity (IEC)

The water absorption capacity of an anion exchange membrane is crucial in order to operate properly in a fuel cell. This parameter is directly related to the Ion Exchange Capacity of the membrane, which in turn depends on the percentage of cationic groups. Therefore, both WU% and IEC will limit the ionic conductivity, as well as the mechanical properties of the material. The WU and the IEC values at room temperature were determined for the different sIPN based membranes and are displayed in Table 3. The effect of functional groups, DC, DCL as well as the effect of the crosslinked polymer/free PSU ratio in the blend are also gathered in Table 3 and Table S2 and S3 of the Supporting Information.

The water uptake values vary as a function of the cationic group and the trend observed is DMIm > MIm > TMA. The polarity, as well as the size of the ionic groups, seem to exert a great influence on this parameter. Although TMA is polar, its size, compared with that of other groups, is small, and therefore it retains less water [47]. Structurally, imidazolium groups are quite similar. For this reason, their water absorption capacities are very close.

Table 3

WU% of functionalized PSU and sIPN membranes.

Membrane	DC%	IEC (mmol g^{-1})	$WU_{20\ °C}$%
sIPN-TMA-OH [a]	87	0.78 ± 0.02	0.9 ± 0.1 [c]
sIPN-MIm-OH [b]	95	1.59 ± 0.01	19 ± 2 [c]
sIPN-MIm-OH [b]	143	2.06 ± 0.04	22 ± 2 [c]
sIPN-DMIm-OH [b]	80	1.51 ± 0.01	10 ± 1 [c]
PSU-TMA-OH [39]	–	1.08	150
PSU-MIm-OH [49]	104	–	60
PSU-MIm-OH [42]	135	2.46	93

WU values are relatively low in all membranes, i.e., in all the cases, the values are lower than 35%, but in general these values are significantly higher when both parameters: the DC and the DCL% increase. The first parameter contribution can be easily explained taking into account that the cationic group anchored to the backbone increases polarity. The second parameter contribution could be related to the increase in polarity due to the presence of TMEDA, a diamine with two aliphatic nitrogen atoms with high hydration ability.

Increasing charge concentration, i.e. IEC, favours the solvation energy of ion pairs, which leads to a significant increase in water uptake. The ratio crosslinked polymer/free PSU has a direct effect in both WU% and IEC parameters (Table S3). Thus, WU and IEC values are higher as the hydrophilic part increased. It is directly related to the polarity increment.

In addition, as shown in Table 3, the absorption capacity of water of the sIPN membranes is remarkably suppressed when compared to that observed for simple functionalized membranes based on PSU, due to the presence of crosslinked polymeric network [48]. The non-crosslinked PSUs present disproportionate WU values (150% in the case of PSU-TMA-OH). However, the blend composed of crosslinked PSU/PSU is able to restrict the absorption of water in the membrane to a greater extent than the non-crosslinked PSU. In those sIPN membranes, composed of 40% of free PSU, the percentage of functional groups is lower than in functionalized simple PSU. For this reason, WU values in the blends are also lower. Our amphiphilic sIPN membranes offer a solution to this issue, since the hydrophobic part clearly limits water uptake.

4.5. Ionic conductivity of sIPN AEMs in aqueous solutions

The ionic conductivity of the different sIPN membranes prepared is determined by Impedance Spectroscopy. Depending on the DC, two different behaviours are found in the Nyquist plots. As an example, Fig. 3A and B shows typical Nyquist plots (-Z_{img} versus Z_{real}) of the AEMs with two different DCs: (A)111% and (B) 58%. The membrane considered here is sIPN-TMA-OH with crosslinked polymer/PSU ratio of 6/4 and 20% of DCL. The experiments were carried out at a given KOH concentration. In the case of high DC (Fig. 3A), three semicircles are distinguished, and it could be an indication of the presence of three different relaxation processes taking place in the electrolyte/membrane system. The high frequency arc (HFA) is not distorted, therefore it could be attributed to the electrolyte solution. This semicircle is reproduced by a RC element. This behaviour is consistent with the fact that the equivalent circuit for the electrolyte solution contains an ideal capacitor [50]. The low frequency arc (LFA) is clearly distorted, denoting a more complex system with different relaxation times. In this case, the experimental data is fitted by considering a circuit with a parallel association of a resistance (R_2) and a Warburg impedance (W) [41]. The third semicircle could be associated to diffusion processes of ions in this electrolyte/membrane system, and it is reproduced considering an R_3 and a Warburg impedance (W) [41]. Meanwhile, the Nyquist plot for membranes with a DC of 58% (Fig. 3B) only has two semicircles. Again, the HFA is not distorted, and it is associated to the electrolyte solution. It is noteworthy that the relative size of the arc at low frequency changed drastically with the DC, and thus could be associated with the membrane. This falls in agreement with the fact that the functional group greatly influences the electrochemical behaviour of the membranes. This influence modifies the associated circuit type according to the transport process, and according to the effect that the sulfonation degree produced in PEMFCs [41]. In this plot, the third contribution could be masked because of a contribution that corresponds to the membrane, and this results in having only one relaxation time for this part of the system.

The previous attributions are verified by using different liquid electrolytes at the same concentration. The Bode plot (-Z_{img} versus

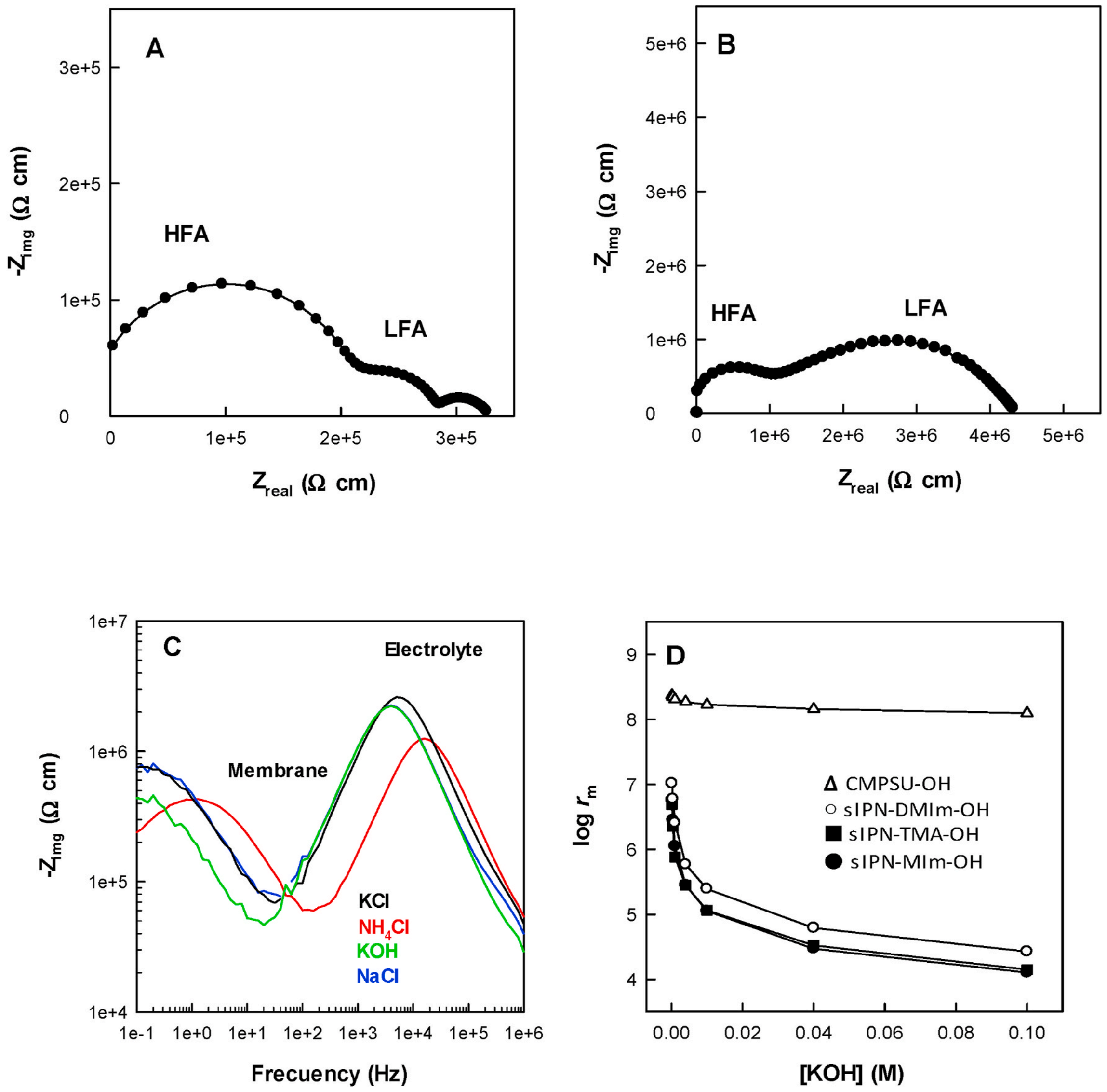

Fig. 3. Nyquist diagrams for (A) sIPN-TMA-OH 111%, and (B) sIPN-TMA-OH 58% membranes at 10^{-2} M [KOH]. (C) Bode diagram for sIPN-MIm with different liquid electrolytes at [KOH] = 4×10^{-4} M and R.T. and equivalent circuits for the different membrane/solution systems. (D) Ionic resistivity of the following membranes: CMPSU (Δ), and sIPN functionalized with TMA (■), MIm (●), and DMIm (○) at different concentrations of KOH and R.T.

frequency) allows the determination of the frequency interval associated with each relaxation process. A similar behaviour is observed in all the membranes studied here. As an example, the Bode plots of the membrane sIPN-MIm obtained in different salts, at a concentration of 4×10^{-4} M, are shown in Fig. 3C. As previously described, the high frequency part ($10^3 < f$ (Hz) $< 10^6$) could be attributed to the liquid electrolyte, while the membrane contribution (LFA) could be observed in the low frequency range ($1 < f$ (Hz) $< 10^3$). The resulting Bode plots are shifted, as a function of the used salt, in the frequency range associated to the liquid electrolyte between $10^3 < f$ (Hz) $< 2 \times 10^4$, while they coincide at the frequency associated with the membrane ($f = 10^2$ Hz).

Most of the electrolytes employed are composed of Cl^- as a counter anion, except for the case of KOH which the anion is OH^-. So, the contribution of the liquid electrolyte depends on three possible factors: the ionic mobility of the counter anion, its size, and the dissociation degree of the salts. As a result, the ionic conductivity of the membrane, immersed in these salts, shows the tendency NH_4Cl > KCl > KOH > NaCl. This tendency would explain the effect that the liquid electrolyte has on the electrochemical properties of the membranes. A similar conclusion was reached for sulfonated PSUs with different sulfonation degrees, by using NaCl to distinguish between the contribution of both the membrane and the liquid electrolyte on the measured ionic conductivity [17,41]. In this case, the relaxation process of both the membrane and the electrolyte solution is in the range $10 < f$ (Hz) $< 6 \times 10^4$, and f (Hz) $> 6 \times 10^4$ Hz, respectively. Therefore, a certain similarity can be observed between the behaviour of sulfonated and chloromethylated PSUs in aqueous media.

The evolution of the ionic resistivity of the membranes (r_m), containing different cationic groups, are plotted as a function of [KOH] in Fig. 3D. This value has been calculated as the inverse of the ionic conductivity of the membranes. The non-functionalized membrane (CMPSU) is chosen as a reference since it does not have the cationic groups responsible for the OH^- transport, and thus its ionic conductivity will is negligible (10^{-6} mS cm^{-1}) for the different KOH concentrations. However, for all membranes based on sIPNs, the resistivity values are considerably lower and decrease as the KOH concentration increases from 10^{-4} to 10^{-1} M. This indicates the great influence that the electrolyte solution, embedded in the membrane network, has on the electrochemical properties of this polymeric material [41,50,51]. The lowest

r_m values are achieved for the membrane with MIm groups in the polymer chain. This is probably due to the higher IEC value (IEC for sIPN-MIm-OH with DC = 143%, DCL = 5% and crosslinked polymer/-PSU 9/1 was 2.60 mmol g^{-1}). Although a similar conduct is observed with the rest of cationic groups. The ionic conductivity (σ_m) of sIPN-based membranes, with different ionic groups (Table 4), does not vary significantly. These membranes, functionalized with imidazolium groups, show higher ionic conductivity than those functionalized with TMA. These results could be due to the water absorption capacity of the membranes (Table 3). The sIPN-TMA membranes show much lower WU percentages compared to the membranes with imidazolium, and this could exert a negative effect in the transport of the hydroxide ions in the medium. Thus, the highest ionic conductivity value is obtained for sIPN-MIm-OH with the crosslinked polymer/PSU ratio of 9/1.

Table 5 shows the ionic conductivity measured (σ_m) for a sIPN membrane and for functionalized PSUs with several ionic groups in the same experimental conditions. Both types of membranes exhibit a similar electrochemical behaviour.

Moreover, the activation energy (E_a), associated with the ion transport mechanism, is obtained from the ionic conductivity measured at different temperatures. The effect that the temperature has, on the ionic conductivity of the membranes, is shown in Fig. 4. As shown in this figure, the ionic conduction in sIPN membranes obeys the Arrhenius law, thus obtaining the following activation energy values of. 21, 20 and 34 kJ mol^{-1} for TMA, MIm, and DMIm groups, respectively. A similar behaviour has been reported in PSU membranes containing pendant DABCO groups (21 kJ mol^{-1}) [16]. These values, in addition to those of the conductivity, indicate that OH^- transport is more impeded in membranes with the DMIm functional group.

4.6. Alkaline stability

The fuel cell performance is also clearly influenced by the alkaline stability of the AEM. The functional group anchored to the backbone of the membrane is susceptible to be degraded in alkaline media, but in turn is responsible for the ionic conductivity of the material. So, if the functional group is degraded over time, the fuel cell performance will drastically decrease.

Alkaline stability is determined through the variation of the ionic conductivity ($\Delta\sigma_m$) once the membranes are treated in a 1 M KOH solution for different times. This variation is the ratio of the hydroxide conductivity measured at a given time (σ) to the hydroxide conductivity at the initial state (σ_o). A value close to 100 implies that the membrane in question does not degrade in this medium. The measurements are carried out by impedance spectroscopy using a home-made cell in alkaline solutions as previously described. The values of $\Delta\sigma_m$ obtained for sIPNs and functionalized-PSUs with different functional groups are shown in Table 6.

The results confirm the high thermal and chemical stability of the TMA group previously described [52,53]. This is associated to the absence of hydrogens in β positions with respect to the nitrogen atom which are implied in the Hofmann elimination. However, this functional group is still susceptible to OH^- nucleophilic attacks [31,54]. Imidazole groups can be a good alternative due to their dimensional stability and exceptional ionic conductivity. Although the sIPN membrane with MIm showed the highest ionic conductivity, it is also the membrane which exhibited the lowest alkaline stability (Table 6). The presence of an acid hydrogen in the carbon, that is located between both nitrogen atoms of the pentagonal ring, which can be removed easily in alkaline media, could explain the poor stability of this group [55]. Meanwhile the DMIm group has a methyl group anchored to the carbon which could impede the OH^- attack, thus preventing degradation. This explains the great alkaline stability of these membranes noted even after 336 h of testing.

Table 4
Ionic conductivity of the membranes measured in KOH (DC<100%).

DCL	sIPN-TMA-OH σ_m (mS cm^{-1})		sIPN-MIm-OH σ_m (mS cm^{-1})		sIPN-DMIm-OH σ_m (mS cm^{-1})	
	Crosslinked polymer/PSU					
	6/4	9/1	6/4	9/1	6/4	9/1
20%	0.01	–	–	–	–	–
15%	–	–	0.05	0.09	0.02	–
5%	–	–	0.06	0.05	0.04	0.03
0%	–	–	0.08	0.11	0.03	0.04

R.T., $f = 10^2$ Hz and [KOH] = 10^{-1} M.

Table 5
Ionic conductivity of sIPN and functionalized polysulfones in a 0.1 M KOH solution.

Membrane	σ_m (mS cm^{-1})
sIPN-MIm-OH 95%	0.06
PSU-TMA-OH 100%	0.09
PSU-BIm-OH 100% [17]	0.19
PSU-DABCO-OH 86% [16]	0.16

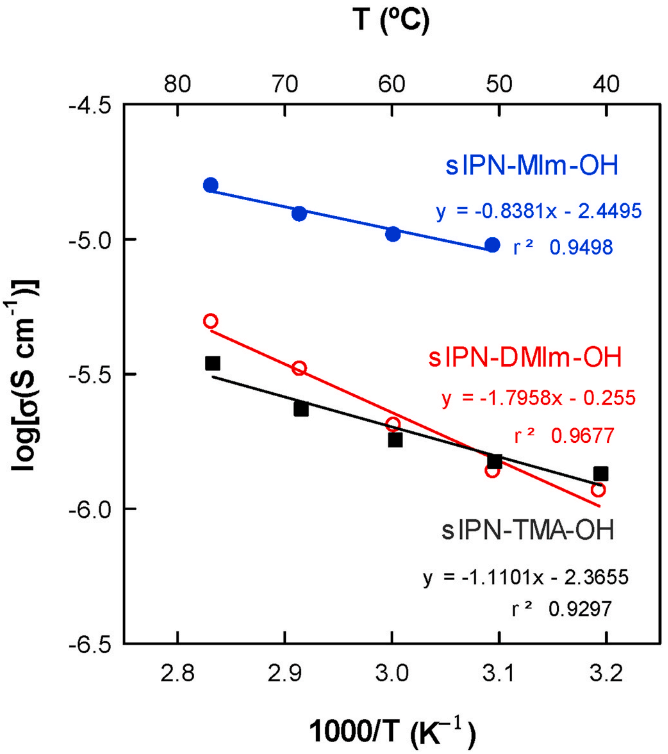

Fig. 4. Evolution of the ionic conductivity as a function of temperature for the prepared membranes at $f = 10^2$ Hz and [KOH] = 10^{-3} M.

Table 6
Values of $\Delta\sigma_m$ for functionalized PSU and sIPNs (DC = 100 and 80%) treated in [KOH] = 1 M at R.T

Time (h)	$\Delta\sigma_m = (\sigma/\sigma_o)$ %					
	sIPN-TMA	sIPN-MIm	sIPN-DMIm	PSU-TMA	PSU-BIm	PSU-DABCO
24	100	100	100	100	100	100
48	99	90	100	96	70	93
72	99	80	100	93	65	87
96	99	75	100	90	61	87
168	–	–	99	–	–	–
336	–	–	87	–	–	–

4.7. Mechanical properties

Dynamic mechanical analysis (DMA) is used to analyse the mechanical properties of sIPN-based membranes. Fig. 5 shows the Stress-Strain curves obtained for PSU-TMA-OH and sIPN-TMA-OH membranes chosen as an example and are compared with starting materials (PSU and CMPSU) in hydrated conditions. PSU membrane shows the higher tensile strength (TS) above 60 MPa. CMPSU exhibits similar rigidity but lower than that of PSU. It could be due to the breakage of the backbone when the chloromethylation reaction takes place [56]. Furthermore, after functionalization with cationic groups, the TS of the resulting membranes decreases (40-30 MPa). If we evaluate the effect that the crosslinked structure has on the mechanical properties of the membrane, the sIPN system (sIPN-TMA-OH 80% TS = 36 MPa) shows higher TS value than the simple one (PSU-TMA-OH 80%, TS = 30 MPa) selected as an example and measured under the same experimental conditions.

The membrane denoted as sIPN-TMA with a DC of 100% and a DCL of 20% is used for a complete study (variation of the crosslinked polymer/PSU ratio, counter ion and hydration conditions, see Table S4). As expected, TS decreases as the crosslinked polymer proportion increases. This is due to the breakage of the backbones in the chloromethylation reaction [56]. Nevertheless, the TS values are quite high even in the extreme case (crosslinked polymer/PSU, 9/1). The influence that the counter ion has on TS value shows a clear trend in all TMA-functionalized membranes studied. Membranes in the Cl^- form reach higher TS values than those observed for OH^- membranes probably due to the effect that the water, retained in the membranes containing the OH^- ions, exerts on the TS. It can be also due to the effect of CO_2 (presence of HCO_3^-, and CO_3^{2-}), but it was not measured. Narducci et al. observed that there was an influence of the counter ion (Cl^-, OH^-, HCO_3^-, and CO_3^{2-}), as well as the hydration effect, on the mechanical properties of the membranes based on PSU modified with TMA and DABCO [57]. So the CO_2 effect on the decrease in TS can not be ruled out. They ascribed the water plasticizing effect to a decrease in van der Waals interactions between backbones, as induced by it is high dielectric constant.

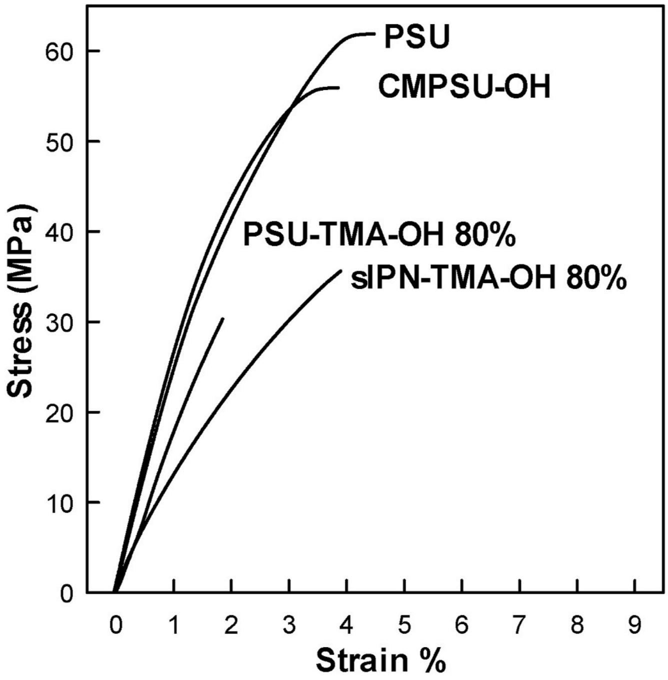

Fig. 5. Stress-Strain curves of PSU, CMPSU-OH, PSU-TMA-OH, and sIPN membranes: Crosslinked polymer/PSU (6/4). Crosslinking Degree 15%. Tests are performed on membranes in the hydroxide form at 30 °C and they are immersed in water before testing.

Given that membranes in the Cl^- form show higher TS, the analysis of the mechanical characteristics of imidazolium-functionalized membranes is performed with samples containing Cl^- as counter ions. Table 7 shows the TS and elongation at break (ε) values for membranes prepared from MIm-and DMIm-functionalized PSU at different DC and DCL values. Mechanical behaviour of the membranes with DC higher than 100% and 9/1 proportion could not be analysed in some cases due to their fragility.

As shown in Table 7, TS and ε values show a dependence on the DC, the DCL and the nature of the cationic group. The effect that both crosslinking process and percentage of crosslinked polymer in the network have on the membrane mechanical properties is less significant than the degree of chloromethylation and the nature of the cationic group. Thus, no clear tendency is observed for TS when DCL varies from 0 to 15% or when the proportion of crosslinked polymer is modified from 6/4 to 9/1 in all samples analysed.

Membranes with a DC < 100% exhibit high TS values, i.e., they were between 32 and 58 MPa for a 6/4 ratio and MIm as a functional group. This parameter ranged between 44 and 54 MPa when the cationic group is replaced by DMIm. These results reveal the high rigidity of the blend due to both, the crosslinked structure, and the nature of the cationic group containing a rigid imidazolium ring. The elongation at break values are not superior of 10% The ductility of the membranes is low due probably to the complex network.

Highly functionalized membranes which contain a DC > 100% show TS values ranged between 24 and 44 MPa for MIm-functionalized membranes at a ratio of 6/4 and ε values are inferior of 4%.

Table 8 shows the comparison of TS and ε for sIPN membranes (with TMA, MIm, and DMIm), but also with functionalized PSU and sIPNs found in literature. The stiffness of the membranes functionalized with quaternary ammonium groups is slightly lower than the value obtained for the imidazolium-functionalized membranes.

Those composed of DMIm show the greater mechanical behaviour.

For comparison with our membranes based on sIPNs, mechanical parameters of membranes of MIm-functionalized PSU are shown in Table 8. Tensile strength values are higher in sIPN membranes due possibly to (i) the presence of free PSU with excellent mechanical strength, and (ii) the attractive forces between polymer backbones, including dipole-dipole interaction (and hydrogen bonding), induction forces, dispersion, or London forces between non-polar molecules [58]. After crosslinking, the process decreases the space between the polymer chains, which, in turn, increases the intermolecular forces and, consequently improve the mechanical characteristics of the membranes. When compared sIPN membranes based on PSU-TMA and polystyrene (PS) or poly(styrene-*co*-divinylbenzene) (PS-*co*-DVB) crosslinked, our sIPN shows a mechanical behaviour noticeably improved by modifying the structure, but also the functional group (Table 8). These results are consistent with the great dimensional stability of our membranes (Table 3). This fact ensures that the dimensional changes during fuel cell operation due to the membrane swelling in different hydration conditions will be reduced. Therefore, mechanical stability of the sIPN membranes guarantees the performance in the final device since the conditions to be exposed does not overcome the experimental ones.

Fig. 6 shows a typical DMA curve for a sIPN membrane which contains MIm groups in Cl^- form in dry conditions, a crosslinked polymer/PSU ratio 6/4, and a degree of crosslinking of 15%. From this graph the relaxation processes can be identified, by means of a decrease of storage modulus and a peak of loss modulus. A slight increase of storage modulus with the temperature is observed. This fact can be attributed to a loss of residual solvent molecules (water and NMP). The bump which appears in the loss modulus curve above 150 °C would indicate an intermediate relaxation [57]. The first peak observed at 180 °C can be attributed to the T_α for the free PSU presented in the polymer matrix since T_g of PSU is around 186 °C. However, the second peak at 200 °C can be associated with the T_α for the crosslinked polymer which has both

Table 7
Tensile strength (TS) and elongation at break (ε) values for dry membranes based on sIPNs in the Cl$^-$ form.

DC	DCL	sIPN-MIm				sIPN-DMIm			
		6/4		9/1		6/4		9/1	
		TS (MPa)	ε %	TS (MPa)	ε %	TS (MPa)	ε %	TS (MPa)	ε %
<100%	15%	32 ± 3	5 ± 1	43 ± 3	2.2 ± 0.3	–	–	–	–
	5%	49 ± 3	5.3 ± 0.6	42 ± 6	4 ± 1	54 ± 3	7.5 ± 0.7	62 ± 2	7 ± 1
	0%	58 ± 2	7.0 ± 3.0	19 ± 4	1.9 ± 0.4	44 ± 4	4.6 ± 0.5	–	–
>100%	15%	44 ± 1	3.6 ± 0.1	–	–	–	–	–	–
	5%	12 ± 4	1.8 ± 0.9	–	–	4.9 ± 1	0.5 ± 0.1	–	–
	0%	24 ± 2	3.3 ± 0.1	–	–	–	–	–	–

Table 8
Comparison of tensile strength (TS) and elongation at break (ε) values for different dry and hydrated membranes.

Membrane	TS [a] (MPa)	ε [a]%	TS [b] (MPa)	ε [b]%
sIPN-TMA	43 ± 3	2 ± 1	48 ± 1	2.6 ± 0.2
sIPN-MIm	58 ± 2	7 ± 3	–	–
sIPN-DMIm	62 ± 2	7 ± 1	–	–
PSU-MIm [46]	50	3.0	–	–
sIPN-(PS-co-DVB)-TMA [34]	21	5.4	10	12.5

[a] Dry membrane.
[b] Hydrated membrane.

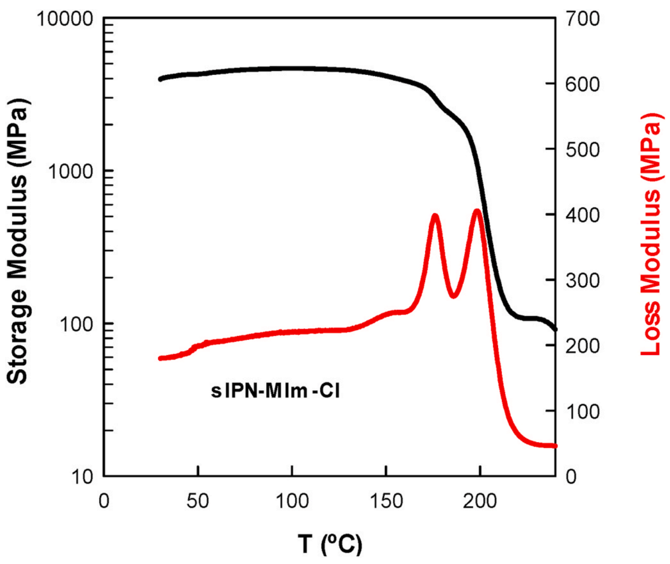

Fig. 6. Dynamic mechanical curves of a MIm-functionalized membrane. Crosslinked polymer/PSU ratio 6/4, degree of crosslinking 15%, and degree of chloromethylation <100%.

the imidazolium group and the crosslinking agent. This value is higher than that observed for the initial polymer, and it can be explained assuming that the crosslinking increases the T_g of the polymer. The covalent crosslinking prevents the chain gliding and retard the glass transition temperature.

The T_g values are similar to those obtained for functionalized PSU with amines such as TMA and DABCO in the chloride form, i.e., T_g (PSU-TMA) = 205 °C, T_g (PSU-DABCO) = 235 °C [54]. The possible plasticizing effect that the water embedded in the polymeric matrix could have on the mechanical behaviour of these membranes is practically negligible. The high dielectric constant of water reduces van der Waals forces between the backbones, which are probed in the elastic domain.

5. Conclusions

In summary, AEMs based on amphiphilic semi-interpenetrating polymer networks for fuel cell applications are successfully synthesized, for the first time. Functionalized PSU is chosen as a rigid and conductive polymer with three different ionic groups (tetramethylammonium, 1-methylimidazolium, and 1,2-dimethylimidazolium) and crosslinked with *N,N,N′,N′*-tetramethylethylenediamine (TMEDA), while free PSU is employed to sustain the mechanical stability of the network. So, the compatibility of the blend is guaranteed by using the same polymer in both components of this blend.

All the chemical structure of the species involved in the synthetic route are characterized by means of ^{1}H NMR and FTIR. The resulting membranes exhibit the following properties: (i) high thermal stability at temperatures lower than 100 °C, (ii) low water uptake at room temperature, (iii) satisfactory ionic conductivity, (iv) excellent chemical stability, and (v) good dimensional stability as a result of the lower water uptake.

Membranes functionalized with 1-methylimidazolium showed the highest ionic conductivity. However, the 1,2-dimethylimidazolium group provokes high thermal and chemical stability since the position susceptible to be attacked by the nucleophile OH$^-$ is blocked. Thus, the degradation of the functional groups is less favoured.

Concerning the durability challenge in AEMFCs, we demonstrate that, just with the addition of a free commercial PSU, it is possible to prepare much more promising materials from the point of view of dimensional stability and mechanical properties. The enhanced stability can be attributed to the covalent crosslinking which can control the water absorption capacity exhibited by these materials (WU% $\leq$ 35% for our membranes whereas the WU values are higher than 100% for non-crosslinked PSU membranes). Thus, the mechanical behaviour of the membranes obtained in the present work exceeds commercial materials even in conditions of extreme humidity and temperature. When compared to the commercial PSU, the difference in TS can be noted to be as low as 10%, and the TS values and the ductility are higher than those obtained with non-crosslinked PSU.

Therefore, the main results obtained from this work reveal that the presence of a hydrophobic segment in the network improves the thermal, alkaline, and dimensional stability of the resulting membranes without deteriorating the ionic conductivity. The membranes based on these semi-interpenetrating networks are outstanding in comparison to functionalized polysulfones. By modifying the proportion of the functional group in the blend, the semi-interpenetrating polymer networks approach can be easily adapted for the preparation of more conductive or stable AEMs. Finally, these results are well-mastered, and can thus be applied to obtain more competitive materials.

Declaration of competing interest

The authors declare that they have no known competing financial interests or personal relationships that could have appeared to influence the work reported in this paper.

Acknowledgements

We thank Agencia Estatal de Investigación (AEI)/Fondo Europeo de Desarrollo Regional (FEDER/UE) for funding the project MINECO (MAT2016-78632-C4-3-R, and PID-2019-106662RB-C43) which supported this work. We also wish to thank the project from the Regional Government (Comunidad de Madrid through PEM4ENERGY-CM-UC3M).

Appendix A. Supplementary data

Supplementary data to this article can be found online at https://doi.org/10.1016/j.polymer.2021.123824.

References

[1] G.F. McLean, T. Niet, S. Prince-Richard, N. Djilali, An assessment of alkaline fuel cell technology, Int. J. Hydrogen Energy 27 (2002) 507–526.

[2] S. Lu, J. Pan, A. Huang, L. Zhuang, J. Lu, Alkaline polymer electrolyte fuel cells completely free from noble metal catalysts, Proc. Natl. Acad. Sci. U.S.A. 105 (2008) 20611–20614.

[3] Q. Hu, G. Li, J. Pan, L. Tan, J. Lu, L. Zhuang, Alkaline polymer electrolyte fuel cell with Ni-based anode and Co-based cathode, Int. J. Hydrogen Energy 38 (2013) 16264–16268.

[4] J.R. Varcoe, P. Atanassov, D.R. Dekel, A.M. Herring, M.A. Hickner, P.A. Kohl, A. R. Kucernak, W.E. Mustain, K. Nijmeijer, K. Scott, T. Xu, L. Zhuang, Anion-exchange membranes in electrochemical energy systems, Energy Environ. Sci. 7 (2014) 3135–3191.

[5] J. Pan, L. Zhu, J. Han, M.A. Hickner, Mechanically Tough and chemically stable anion exchange membranes from rigid-flexible semi-interpenetrating network, Chem. Mater. 27 (2015) 6689–6698.

[6] D. Dekel, Alkaline membrane fuel cells, membranes, in: R. Savinell, K.-I. Ota, G. Kreysa (Eds.), Encyclopedia of Applied Electrochemistry, Springer, Berlin, 2014, pp. 33–45.

[7] X.M. Wu, W.T. Chen, X.M. Yan, G.H. He, J.J. Wang, Y. Zhang, X.P. Zhu, Enhancement of hydroxide conductivity by the diquaternization strategy for poly (ether ether ketone) based anion exchange membranes, J. Mater. Chem. A 2 (2014) 12222–12231.

[8] N. Ziv, W.E. Mustain, D.R. Dekel, The effect of ambient carbon dioxide on anion-exchange membrane fuel cells, ChemSusChem 11 (2018) 1136–1150.

[9] J. Dai, G. He, X. Ruan, W. Zheng, Y. Pan, X. Yan, Constructing a rigid crosslinked structure for enhanced conductivity of imidazolium functionalized polysulfone hydroxide exchange membrane, Int. J. Hydrogen Energy 41 (2016) 10923–10934.

[10] A.D. Mohanty, S.E. Tignor, J.A. Krause, Y.K. Choe, C. Bae, Systematic alkaline study of polymer backbones for anion exchange membrane applications, Macromolecules 49 (2016) 3361–3372.

[11] Y. Pan, T.Y. Wang, X.M. Yan, X.W. Xu, Q.D. Zhang, B.L. Zhao, I. El Hamouti, C. Hao, G.H. He, Novel benzimidazolium functionalized polysulfone-based anion exchange membranes with improved alkaline stability, Chin. J. Polym. Sci. 36 (2018) 129–138.

[12] L. Liu, X. Chu, J. Liao, Y. Huang, Y. Li, Z. Ge, M.A. Hickner, N. Li, Tuning the properties of Poly(2,6-dimethyl-1,4-phenylene oxide) anion exchange membranes and their performance in H_2/O_2 fuel cells, Energy Environ. Sci. 11 (2018) 435–446.

[13] W. Zhang, Y. Liu, J.L. Horan, Y. Jin, X. Ren, S.P. Ertem, S. Seifert, M.W. Liberatore, A.M. Herring, E.B. Coughlin, Crosslinked anion exchange membranes with connected cations, J. Polym. Sci., Part A: Polym. Chem. 56 (2017) 618–625.

[14] G. Shukla, V.K. Shahi, Poly(arylene ether ketone) copolymer grafted with amine groups containing long alkyl chain by chloroacetylation for improved alkaline stability and conductivity of anion exchange membrane, ACS Appl. Energy Mater. 1 (2018) 1175–1182.

[15] D. Zuo, Y. Gong, Q. Yan, H. Zhang, Preparation and characterization of hydroxyl ion-conducting interpenetrating polymer network based on PVA and PEI, J. Polym. Res. 23 (2016) 126–132.

[16] M.T. Pérez-Prior, N. Ureña, M. Tannenberg, C. del Río, B. Levenfeld, DABCO-functionalized polysulfones as anion-exchange membranes for fuel cell applications: effect of crosslinking, J. Polym. Sci., Part B: Polym. Phys. 55 (2017) 1326–1336.

[17] M.T. Pérez-Prior, A. Várez, B. Levenfeld, Synthesis and characterization of benzimidazolium-functionalized polysulfones as anion-exchange membranes, J. Polym. Sci., Part A: Polym. Chem. 53 (2015) 2363–2373.

[18] X. Yan, S. Gu, G. He, X. Wu, W. Zheng, X. Ruan, Quaternary phosphonium-functionalized poly(ether ether ketone) as highly conductive and alkali-stable hydroxide exchange membrane for fuel cells, J. Membr. Sci. 466 (2014) 220–228.

[19] C. Jangu, T.E. Long, Phosphonium cation-containing polymers: from ionic liquids to polyelectrolytes, Polymer 55 (2014) 3298–3304.

[20] L. Liu, Q. Li, J. Dai, H. Wang, B. Jin, R. Bai, A facile strategy for the synthesis of guanidinium-funcionalized polymer as alkaline anion exchange membrane with improved alkaline stability, J. Membr. Sci. 453 (2014) 52–60.

[21] D.S. Kim, C.H. Fujimoto, M.R. Hibbs, A. Labouriau, Y.-K. Choe, Y.S. Kim, Resonance stabilized perfluorinated ionomers for alkaline membrane fuel cells, Macromolecules 46 (2013) 7826–7833.

[22] M.S. Cha, J.Y. Lee, T.-H. Kim, H.Y. Jeong, H.Y. Shin, S.-G. Oh, Y.T. Hong, Preparation and characterization of crosslinked anion exchange membrane (AEM) materials with poly(phenylene ether)-based short hydrophilic block for use in electrochemical applications, J. Membr. Sci. 530 (2017) 73–83.

[23] X.L. Huang, C.X. Lin, E.N. Hu, F. Soyekwo, Q.G. Zhang, A.M. Zhu, Q.L. Liu, Imidazolium-functionalized anion exchange membranes using poly(ether sulfone)s as macrocrosslinkers for fuel cells, RCS Adv 7 (2017) 27342–27353.

[24] X. Gong, X. Yan, T. Li, X. Wu, W. Chen, S. Huang, Y. Wu, D. Zhen, G. He, Design of pendent imidazolium side with flexible ether-containing spacer for alkaline anion exchange membrane, J. Membr. Sci. 523 (2017) 216–224.

[25] K.M. Hugar, H.A. Kostalik, , IV, G.W. Coates, Imidazolium cations with exceptional alkaline stability: a systematic study of structure-stability relationships, J. Am. Chem. Soc. 137 (2015) 8730–8737.

[26] M.A. Hickner, A.M. Herring, E.B. Coughlin, Anion exchange membranes: current status and moving forward, J. Polym. Sci., Part B: Polym. Phys. 51 (2013) 1727–1735.

[27] M.T. Pérez-Prior, T. García-García, A. Várez, B. Levenfeld, Preparation and characterization of ammonium-functionalized polysulfone/Al_2O_3 composite membranes, J. Mater. Sci. 50 (2015) 5893–5903.

[28] J.Y. Chu, K.H. Lee, A.R. Kim, D.J. Yoo, Study on the chemical stabilities of poly (arylene ether) random copolymers for alkaline fuel cells: effect of main chain structures with different monomer units, ACS Sustain. Chem. Eng. 7 (2019) 20077–20087.

[29] E.A. Weiber, P. Jannasch, Anion-conducting polysulfone membranes containing hexa-imidazolium functionalized biphenyl units, J. Polym. Sci. 520 (2016) 425–433.

[30] W. Lu, Z.G. Shao, G. Zhang, Y. Zhao, B. Yi, Crosslinked poly(vinylbenzyl chloride) with a macromolecular crosslinker for anion exchange membrane fuel cells, J. Power Sources 248 (2014) 905–914.

[31] G. Couture, A. Alaaeddine, F. Boschet, B. Ameduri, Polymeric materials as anion-exchange membranes for alkaline fuel cells, Prog. Polym. Sci. 36 (2011) 1521–1557.

[32] N.J. Robertson, H.A. Kostalik IV, T.J. Clark, P.F. Mutolo, H.D. Abruña, G.W. Coates, Tunable high performance cross-linked alkaline anion exchange membranes for fuel cell applications, J. Am. Chem. Soc. 132 (2011) 3400–3404.

[33] P. Kanakasabai, A.P. Deshpande, S. Varughese, Novel polymer electrolyte membranes based on semi-interpenetrating blends of poly(vinyl alcohol) and sulfonated poly(ether ether ketone), J. Appl. Polym. Sci. 127 (2013) 2140–2151.

[34] S.S. He, A.L. Strickler, C.W. Frank, A semi-interpenetrating network approach for dimensionally stabilizing highly-charged anion exchange membranes for alkaline fuel cells, ChemSusChem 8 (2015) 1472–1483.

[35] B. Lin, L. Qiu, J. Lu, F. Yan, Cross-linked alkaline ionic liquid-based polymer electrolytes for alkaline fuel cell applications, Chem. Mater. 22 (2010) 6718–6725.

[36] Y. Ye, Y.A. Elabd, Relative chemical stability of imidazolium-based alkaline anion exchange polymerized ionic liquids, Macromolecules 44 (2011) 8494–8503.

[37] S.J. Peighambardoust, S. Rowshanzamir, M. Amjadi, Review of the proton exchange membranes for fuel cell applications, Int. J. Hydrogen Energy 35 (2010) 9349–9384.

[38] N. Pantamas, C. Khonkeng, S. Krachodnok, A. Chaisena, Ecofriendly and simplified synthetic route for polysulfone-based solid-state alkaline electrolyte membrane, Am. J. Appl. Sci. 9 (2012) 1577–1582.

[39] J. Pan, S. Lu, Y. Li, A. Huang, L. Zhuang, J. Lu, High-performance alkaline polymer electrolyte for fuel cell applications, Adv. Funct. Mater. 20 (2010) 312–319.

[40] S.C. Price, X. Ren, A.C. Jackson, Y. Ye, Y.A. Elabd, F.L. Beyer, Bicontinuous alkaline fuel cell membranes from strongly self-segregating block copolymers, Macromolecules 46 (2013) 7332–7340.

[41] J. Benavente, J.M. García, R. Riley, A.E. Lozano, J. de Abajo, Sulfonated poly(ether ether sulfones). Characterization and study of dielectrical properties by impedance spectroscopy, J. Membr. Sci. 175 (2000) 43–52.

[42] F. Zhang, H. Zhang, C. Qu, Imidazolium functionalized polysulfone anion exchange membrane for fuel cell application, J. Mater. Chem. 21 (2011) 12744–12752.

[43] K. Yang, H. Ni, T. Shui, X. Chi, W. Chen, Q. Liu, J. Xu, Z. Wang, High conductivity and alkali-resistant stability of imidazole side chain crosslinked anion exchange membrane, Polymer 211 (2020) 123085.

[44] H. Li, J. Dong, X. Cao, X. Ren, Z. Hao, J. Yang, Diamine crossklinked anion exchange membranes based on poly(vinyl benzyl methylpyrrolidinium), Polymer 212 (2020) 123156.

[45] H. Ngo, K. LeCompte, L. Hargens, A.B. McEwen, Thermal properties of imidazolium ionic liquids, Thermochim. Acta 97 (2000) 357–358.

[46] J. Yang, Q. Li, J.O. Jensen, C. Pan, L.N. Cleemann, N.J. Bjerrum, R. He, Phosphoric acid doped imidazolium polysulfone membranes for high temperature proton exchange membrane fuel cells, J. Power Sources 205 (2012) 114–121.

[47] C. Yang, S. Wang, W. Ma, L. Jiang, G. Sun, Comparison of alkaline stability of quaternary ammonium- and 1,2-methylimidazolium-based alkaline anion exchange membranes, J. Membr. Sci. 487 (2015) 12–18.

[48] T. Zhu, C. Tang, Crosslinked metallo-polyelectrolytes with enhanced flexibility and dimensional stability for anion-exchange membranes, Polym. Chem. 11 (2020) 4542–4546.

[49] X. Yan, G. He, S. Gu, X. Wu, L. Du, Y. Wang, Imidazolium-functionalized polysulfone hydroxide exchange membranes for potential applications in alkaline membrane direct alcohol fuel cells, Int. J. Hydrogen Energy 37 (2012) 5216–5224.

[50] J. Benavente, X. Zhang, R. Garcia Valls, Modification of polysulfone membranes with polyethylene glycol and lignosulfate: electrical characterization by impedance spectroscopy measurements, J. Colloid Interface Sci. 285 (2005) 273–280.

[51] L. An, T.S. Zhao, Q.X. Wu, L. Zeng, Comparison of different types of membrane in alkaline direct ethanol fuel cells, Int. J. Hydrogen Energy 37 (2012) 14536–14542.

[52] S. Maurya, S.H. Shin, M.K. Kim, S.H. Yun, S.H. Moon, Stability of composite anion exchange membranes with various functional groups and their performance for energy conversion, J. Membr. Sci. 443 (2013) 28–35.

[53] J. Zhou, J. Guo, D. Chu, R. Chen, Impacts of anion-exchange-membranes with various ionic exchange capacities on the performance of H_2/O_2 fuel cells, J. Power Sources 219 (2012) 272–279.

[54] S. Adhikari, M.K. Pagels, J.Y. Jeon, C. Bae, Ionomers for electrochemical energy conversion & technologies, Polymer 211 (2020) 123080.

[55] B. Shen, H. Pu, Poly(ether sulfone)s with pendent imidazolium for anion exchange membranes via click chemistry, Polymer 207 (2020) 122944.

[56] P.P. Yatin, W.L. Jarrett, K.A. Mauritz, Deterioration of mechanical properties: a cause for fuel cell membrane failure, J. Membr. Sci. 356 (2010) 7–13.

[57] R. Narducci, J.F. Chailan, A. Fahs, L. Pasquini, M.L. Di Vona, P. Knauth, Mechanical properties of anion exchange membranes by combination of tensile stress-strain tests and dynamic mechanical analysis, J. Polym. Sci., Part B: Polym. Phys. 54 (2016) 1180–1187.

[58] R. He, Q.F. Li, A. Bach, J.O. Jensen, N.J. Bjerrum, Physicochemical properties of phosphoric acid doped polybenzimidazole membranes for fuel cells, J. Membr. Sci. 277 (2006) 38–45.